Am J Cancer Res 2024;14(7):3565-3583
www.ajcr.us /ISSN:2156-6976/ajcr0156568

Original Article

m^{6}A modification of CDC5L promotes lung adenocarcinoma progression through transcriptionally regulating WNT7B expression

Nanding Yu[1,3*], Yingxiao Wu[1,3*], Qiongying Wei[1,3], Xiaoping Li[1,3], Mengling Li[1,3], Weidong Wu[2,4]

[1]Department of Pulmonary and Critical Care Medicine, Fujian Medical University Union Hospital, Fuzhou 350001, Fujian, China; [2]Department of Thoracic Surgery, Fujian Medical University Union Hospital, Fuzhou 350001, Fujian, China; [3]Department of Geriatric Medicine, Fujian Medical University Union Hospital, Fuzhou 350001, Fujian, China; [4]Fujian Key Laboratory of Cardio-Thoracic Surgery, Fujian Medical University, Fuzhou 350122, Fujian, China. [*]Equal contributors and co-first authors.

Received March 14, 2024; Accepted June 25, 2024; Epub July 15, 2024; Published July 30, 2024

Abstract: Cell division cycle 5-like (CDC5L) protein is implicated in the development of various cancers. However, its role in the progression of lung adenocarcinoma (LUAD) remains uncertain. Our findings revealed frequent upregulation of CDC5L in LUAD, which correlated with poorer overall survival rates and advanced clinical stages. *In vitro* experiments demonstrated that CDC5L overexpression stimulated the proliferation, migration, and invasion of LUAD cells, whereas CDC5L knockdown exerted suppressive effects on these cellular processes. Furthermore, silencing CDC5L significantly inhibited tumor growth and metastasis in a xenograft mouse model. Mechanistically, CDC5L activates the Wnt/β-catenin signaling pathway by transcriptionally regulating WNT7B, thereby promoting LUAD progression. Besides, METTL14-mediated m^{6}A modification contributed to CDC5L upregulation in an IGF2BP2-dependent manner. Collectively, our study uncovers a novel molecular mechanism by which the m^{6}A-induced CDC5L functions as an oncogene in LUAD by activating the Wnt/β-catenin pathway through transcriptional regulation of WNT7B, suggesting that CDC5L may serve as a promising prognostic marker and therapeutic target for LUAD.

Keywords: CDC5L, lung adenocarcinoma, Wnt/β-catenin, WNT7B, METTL14

Introduction

Over the past decades, lung adenocarcinoma (LUAD) has emerged as the predominant histologic subtype of lung cancer, contributing to rising morbidity and mortality rates [1-3]. Extensive research has unveiled numerous genomic alterations associated with LUAD progression, leading to notable advancements in molecularly targeted therapies [4]. Despite these developments, drug resistance and side effects have compromised therapeutic efficacy, resulting in a discouraging overall 5-year survival rate of less than 20% for LUAD patients [5]. Therefore, it is urgent to enhance our understanding of the cellular mechanisms underlying LUAD progression.

The Cell division cycle 5-like (CDC5L) protein shares significant similarity with the Schizosaccharomyces pombe CDC5 gene product, known as a crucial cell cycle regulator essential for the G2/M transition [6, 7]. CDC5L interacts with the cell cycle checkpoint protein ATR, activating downstream effectors including Chk1 and Rad17 [8]. Inhibition of CDC5L disrupts the S phase cell cycle checkpoint, leading to increased drug sensitivity [9]. Besides its role in cell cycle regulation, CDC5L is a component of the spliceosome complex and contributes to pre-mRNA splicing, indicating its multifunctional nature [7, 10, 11]. Notably, CDC5L has been implicated in various human somatic tumors. In colorectal cancer, CDC5L acts as an oncogene, promoting the transcriptional activation of the hTERT promoter [12-14]. Moreover, CDC5L has demonstrated potential oncogenic activity in osteosarcoma and cervical tumors [15-17]. Due to its close association with the mitotic stage of the cell cycle, CDC5L is considered a

https://doi.org/10.62347/QHFA9669

promising target for tumor therapy [6, 7]. However, despite the growing knowledge about CDC5L's involvement in different cancers, its role in lung adenocarcinoma (LUAD) and the underlying mechanisms remain unexplored. Therefore, further investigation is required to understand the significance of CDC5L in LUAD and its potential as a therapeutic target.

Recent research has underscored the importance of RNA modifications, specifically N6-methyladenosine (m^6A) alterations, in regulating gene expression and in the realm of cancer biology [18, 19]. The m^6A modification impacts various biological processes, including tissue development, stem cell maintenance and differentiation, and DNA damage response. Currently, distinct groups of proteins have been identified and validated as writers, readers, and erasers responsible for adding, recognizing, and removing the methyl group from RNA molecules, respectively [20, 21]. Disruption of any of these processes can lead to aberrant expression of target genes, initiating and promoting diseases such as lung cancer, pancreatic cancer, glioblastoma, and breast cancer. Therefore, m^6A modification holds promise as potentially valuable diagnostic biomarkers and therapeutic targets for tumorigenesis, invasion, metastasis, and drug resistance [22-26]. Our aim is to explore the impact of m^6A modification on the enhancement of CDC5L expression in LUAD cells. Delving into the epigenetic control of CDC5L through m^6A modification could offer fresh perspectives on LUAD pathogenesis and unveil promising targets for therapeutic interventions.

Highly conserved pathways, Wnt signaling pathways are recognized for their pivotal role in both embryonic tissue development and adult tissue maintenance. Dysregulated Wnt signaling has been linked to the pathogenesis of numerous cancers. Activation of the Wnt pathway stabilizes β-catenin, prompting its translocation to the nucleus and subsequent transcriptional activation of target genes crucial for cell proliferation, survival, and invasion [27-29]. The Wnt/β-catenin signaling pathway significantly influences the development and advancement of diverse cancers. Numerous investigations have substantiated its involvement in lung cancers, such as LUAD. Within LUAD, abnormal Wnt pathway activation has been detected, correlating with tumor proliferation, metastasis, and unfavorable prognosis [30-33]. A constitutively activating mutation of β-catenin was discovered in lung cancer clinical samples, initiating a signaling cascade centered around β-catenin as the pivotal component, consequently fostering tumorigenesis. Despite some noncanonical Wnt proteins being implicated in tumorigenesis signaling dysfunction, the role of noncanonical Wnt signaling in lung cancer remains contentious. The potential of CDC5L to stimulate the Wnt/β-catenin signaling pathway and thereby facilitate LUAD progression has yet to be investigated. However, there are multiple limitations in our current study. Firstly, the interaction between CDC5L and the Wnt/β-catenin pathway is primarily supported by in vitro experiments and lacks in vivo validation. Secondly, while our findings are promising, they are based on a single preclinical model. Further validation in additional preclinical models is essential to confirm the robustness and generalizability of our results. Additionally, extrapolating our findings to clinical cohorts requires caution, as the complexities of human biology may differ from the animal models utilized. By addressing these limitations, we can provide a more balanced perspective on the implications of our research.

In summary, our study comprehensively investigated the expression and clinical significance of CDC5L as a potential biomarker in LUAD. We validated CDC5L's oncogenic roles through experiments and confirmed its potential as a prognostic biomarker. It is crucial to explore the clinical implications of targeting CDC5L and the Wnt/β-catenin pathway in LUAD treatment. By targeting these components, there is potential to disrupt crucial oncogenic signaling pathways, offering promising avenues for therapeutic intervention. However, several challenges must be addressed. Firstly, understanding the precise mechanisms by which CDC5L interacts with the Wnt/β-catenin pathway in LUAD progression is essential for developing targeted therapies. Additionally, developing effective inhibitors or modulators that can selectively target CDC5L or components of the Wnt/β-catenin pathway with minimal off-target effects remains challenging. Moreover, given the complexity and heterogeneity of LUAD, personalized therapeutic approaches accounting for individual variations in pathway activation and tumor characteristics may be necessary for

optimal treatment outcomes. Future directions for therapeutic development may include investigating combination therapies targeting multiple nodes within the Wnt/β-catenin pathway or integrating targeted therapies with immunotherapy to enhance efficacy. In conclusion, while targeting CDC5L and the Wnt/β-catenin pathway shows promise for LUAD treatment, further research is essential to overcome challenges and translate these findings into clinical benefits for patients.

Materials and methods

Patient tissue samples

LUAD tumor samples and corresponding adjacent normal tissue were collected from the Union Hospital affiliated to Fujian Medical University. Samples were snap frozen and stored at -80°C until use. In addition, we conducted immunohistochemical staining of formalin-fixed paraffin-embedded LUAD patient samples and normal control samples. All patients were diagnosed with LAD (stages I, II, III, and IV) according to histopathological evaluation. The Research Ethics Committee of the Union Hospital affiliated to Fujian Medical University approved this study, which was consistent with the Declaration of Helsinki. All patients provided written informed consent.

Cell lines and cell culture

LUAD cell lines (A549, SPCA1, PC9, H1299, H1975, H23) and human bronchial epithelial cell (HBE) were purchased from the Cell Bank of Type Culture Collection of the Chinese Academy of Sciences, Shanghai Institute of Cell Biology (Shanghai, China). H1975, H23, SPCA1 and HBE cells were cultured in DMEM medium (Gibco), and PC9, A549 and H1299 cells were cultured in RPMI 1640 medium (Gibco), supplemented with 10% fetal bovine serum. All cells were cultured at 37°C in a humidified incubator containing 5% CO_2.

RNA extraction, reverse transcription, and qRT-PCR

Total RNA was extracted from cultured cells using TRIzol reagent (Thermo) according to the manufacturer's instructions. The extracted RNA was dissolved with RNAase-free water, and 1 μg RNA from each sample was used for cDNA synthesis using a Reverse Transcription Kit (Takara). SYBR Select Master Mix (Applied Biosystems) was used for qRT-PCR. The qRT-PCR primers for CDC5L, WNT7B, CCND1, cMyc, Axin2 and GAPDH were designed using Primer Express version 5.0 software (Applied Biosystems). The comparative CT method (ΔΔCT) was used to measure the relative gene expression. CDC5L Forward Primer: 5'-GACCTGGCTGTGCTATGG-3'; CDC5L Reverse Primer: 5'-TGCTGCTGCTGAACCTTC-3'; WNT7B Forward Primer: 5'-AGGCAGTGAGGACATCGAAA-3'; WNT7B Reverse Primer: 5'-GCCTTCTGGTCCTTTCCTCA-3'; CCND1 forward primer: 5'-AGTTGTTGGGGCTC CTCAG-3'; CCND1 reverse primer: 5'-AGACCTTCGTTGCCCTCTGT-3'; cMyc Forward Primer: 5'-GCAAACACAAACCTGTCTCC-3'; cMyc Reverse Primer: 5'-AGGTAGTGGATGATGATGTTCTG-3'; Axin2 Forward Primer: 5'-TCTTTGCGAGATGCTTCTGC-3'; Axin2 Reverse Primer: 5'-TTCCATCTCTGCGTTGCTTC-3'; GAPDH Forward Primer: 5'-TGCACCACCAACTGCTTA-GC-3'; GAPDH Reverse Primer: 5'-GGCATGGACTGTGGTCATGAG-3'.

Immunohistochemistry (IHC)

Paraffin-embedded sections were deparaffinized and incubated in retrieval buffer solution for antigen retrieval. The sections were incubated with corresponding antibodies: anti-CDC5L (Abcam, ab129114, 1:100).

EdU staining

5×10^5 cells were seeded in a 6-well plate and cultured overnight. Then, 20 μM EdU working solution (Beyotime) was added to each well in a 1:1 volume, resulting in a final concentration of 10 μM. After a 2-hour incubation at 37°C, the culture was terminated and fixed with room temperature methanol for 15 minutes. Next, methanol was removed, and 500 μL of 0.2% Triton X-100 was added to each well for cell permeabilization. Cells were gently shaken at room temperature for 10 minutes. The dyeing reaction solution was prepared according to the manufacturer's instructions, and 100 μL of the reaction solution was added to each well. The plates were incubated in the dark at room temperature for 30 minutes with gentle shaking to trigger the click reaction. Nuclei staining was performed using Hoechst-33342 dye (Thermos). Finally, images were captured using

an FV3000 Fluorescence Confocal Microscopy (Olympus).

Western blotting

Western blotting was performed according to standard protocols as previously described [34]. Briefly, tissues or cultured cells were lysed with lysis buffer (RIPA, KeyGEN) containing protease inhibitors (PMSF, KeyGEN) on ice, and protein concentration was determined using a BCA Kit (KeyGEN). Western blotting was obtained utilizing 30 μg of lysate protein. The antibodies used were as follows: anti-CDC5L (Abcam), anti-Axin2 (Thermo), anti-CyclinD1 (Cell Signaling Technology), anti-cMyc (ThermoFisher), anti-GAPDH (Cell Signaling Technology).

Cell transfection and stable cell line construction

Lentiviruses expressing CDC5L and hairpin-derived small RNAs (shRNAs) targeting CDC5L or WNT7B were obtained from General Biosystems (Anhui, China). After 72 hours of lentivirus infection, cells were treated with 2.5 μg/ml puromycin to select for stable infection. Small interfering RNAs (siRNAs) targeting METTL14, IGF2BP1, IGF2BP2, and IGF2BP3 (General Biosystems, Anhui, China) were transfected into LUAD cells using Lipofectamine RNAiMAX following the manufacturer's protocol (Invitrogen; Thermo Fisher Scientific). Detailed sequences of shRNAs and siRNAs can be found in Table S1.

Cell proliferation assay

In the Cell Counting Kit-8 (CCK-8) assay, cells were seeded in 96-well plates at a density of 4000 cells/100 μL. The absorbance at 450 nm was measured using an ELx-800 Universal Microplate Reader.

Migration and invasion assay

For the Transwell assay, 8 μm PET inserts (24-well Millicell) or Matrigel-coated membranes (BD Biosciences) were placed in the upper chamber. The upper chamber was then filled with 200 μL of serum-free medium, while the lower chamber was filled with 800 μL of serum-containing medium. A total of 5 × 10^4 cells were added to the upper chamber. After 24 hours (for migration) or 48 hours (for invasion), the cells in the lower chamber were fixed and stained.

Wound healing assay

Wound healing assay was performed as previously reported [34-37], with 10 μg/mL mitomycin (Sigma) treated for 2 h, the 100% confluent monolayers of LUAD cells were scratched and washed three times with PBS. The marked areas were captured before and after scratch for 24 h.

RNA-seq analysis

Total RNA was extracted from control and CDC5L-knockdown H1299 cells using TRIzol reagent (Invitrogen, Carlsbad, CA, USA), following the manufacturer's protocol. The RNA was subjected to reverse transcription using the SMARTer Ultra Low RNA Kit (Clontech). Subsequently, cDNA amplification was performed using the Advantage 2 PCR Kit (Clontech) according to the manufacturer's instructions. To create cDNA libraries, the KAPA Stranded mRNA Seq Kit (KAPA) was employed, following the manufacturer's guidelines. Sequencing was conducted on the Illumina HiSeq2500 platform, generating paired-end reads with a read length of 150 bp.

Luciferase reporter assay

The promoter region of WNT7B was amplified and inserted into the luciferase reporter plasmid (pGL3-basic). These luciferase reporter plasmids were co-transfected with CMV-CDC5L expression plasmids, while CMV-empty vector was used as negative controls. CMV-Renilla plasmid served as an internal control, and the Firefly/Renilla value was utilized to measure luciferase activity. After 48 hours of transfection, cells were harvested and assessed for luciferase activity using the Dual Luciferase Reporter Assay System (Promega).

Animal studies

Male athymic BALB/c mice (5-weeks-old) were purchased from SPF (Beijing) Biotechnology Co., Ltd. 1×10^7 LUAD tumor cells in 100 μL sterile PBS were injected subcutaneously to each mouse and tumors were harvested at 30 days after injection. Tumor volumes were mea-

sured with an external caliper, and calculated using the equation (L × W2)/2. Tumors were measured every 5 days and harvested at 30 days after injection. All animal studies were conducted in accordance with NIH animal use guidelines and protocols were approved by animal care committee of Union Hospital affiliated to Fujian Medical University.

Lung metastasis model of LUAD

To investigate the metastasis of LUAD cell *in vivo*, intravenous injection of 1 × 10^6 H1299 and H1975 cells into the lateral tail vein of 5-week-old BALB/c nude mice. Tumor colonies were examined in the lungs on day 30. Mice were sacrificed and the lung tissues were collected, dissected, and stained with H&E. The tumor colonies histomorphology was photographed, and the percentage occupancy of metastases was calculated. All animal studies were conducted in accordance with NIH animal use guidelines and protocols were approved by animal care committee of Union Hospital affiliated to Fujian Medical University.

mRNA stability

To assess RNA stability in LUAD cells, we treated the cells with 5 μg/ml actinomycin D (Act-D, Sigma). Following the specified incubation times, cells were harvested and RNA was isolated for qRT-PCR analysis. The mRNA half-life ($t_{1/2}$) of CDC5L was determined using the formula ln2/slope, with GAPDH serving as the normalization reference.

RNA immunoprecipitation

RNA immunoprecipitation (RIP) experiments were conducted using the Magna RIP RNA-Binding Protein Immunoprecipitation Kit (Millipore, Bedford, MA, USA). Antibodies for RIP assays targeting IgG, IGF2BP2, and m^6A were diluted at a ratio of 1:1000. Following RIP, RNA concentrations were quantified utilizing the Qubit® RNA High-sensitivity (HS) Assay Kit and Qubit 2.0. The co-precipitated RNAs were identified through reverse transcription (RT)-PCR analysis, with RNA expression levels normalized to the total RNA input for reverse transcription.

Statistical analysis

Data are presented as mean ± SEM. Statistical analyses were performed with Graphpad Prism software (version 9.1.4). Statistical significance was compared via unpaired Student's *t* test or one-way analysis of variance (ANOVA) followed with Bonferroni's multiple as appropriate. Differences were considered statistically significant at the level of $P < 0.05$.

Results

CDC5L was overexpressed in LUAD and correlated with worse prognosis

Gene expression profiling interactive analysis (GEPIA) showed that the expression of CDC5L in LUAD significantly increased in tumor compared with normal lung tissue (**Figure 1A**). Next, we determined whether CDC5L expression in LUAD tissues was associated with clinicopathological features of patients in TCGA dataset. As shown in **Figure 1B**, high CDC5L expression was significantly associated with TNM stage ($P < 0.05$). To further validate the results found in TCGA, we investigated the expression of CDC5L in patient samples. Compared with normal lung tissues, the protein level of CDC5L is highly expressed in LUAD tissue (**Figure 1C**, **1D**). Then, we measured the expression of CDC5L in LUAD cell lines (A549, SPCA1, PC9, H1299, H1975, H23) and human bronchial epithelial cell (HBE) cells. CDC5L was upregulated in LUAD cell lines, especially in H1299 and H1975 (**Figure 1E**, **1F**). Those data suggested that CDC5L was a potential oncogene in LUAD.

CDC5L promotes proliferation and migration of LUAD in vitro

To investigate the role of CDC5L in LUAD progression, we utilized lentivirus carrying short-hairpin RNA (shRNA) targeting CDC5L (shCDC5L) to infect H1299 and H1975 cells. Western blot confirmed the expression of CDC5L was robustly knocked down in both H1299 and H1975 (Figure S1A). Cell viability was assessed using the CCK-8 assay at different time points (0, 1, 2, and 3 days) post-infection. Our results demonstrated that H1299 and H1975 cells infected with shCDC5L exhibited significantly decreased cell viability compared to the vector control (**Figure 2A**). We further conducted transwell and wound healing assays to evaluate the impact of CDC5L knockdown on cell migration and invasion in LUAD cells. The findings revealed that down-regulation of CDC5L suppressed cell migration and invasion in LUAD

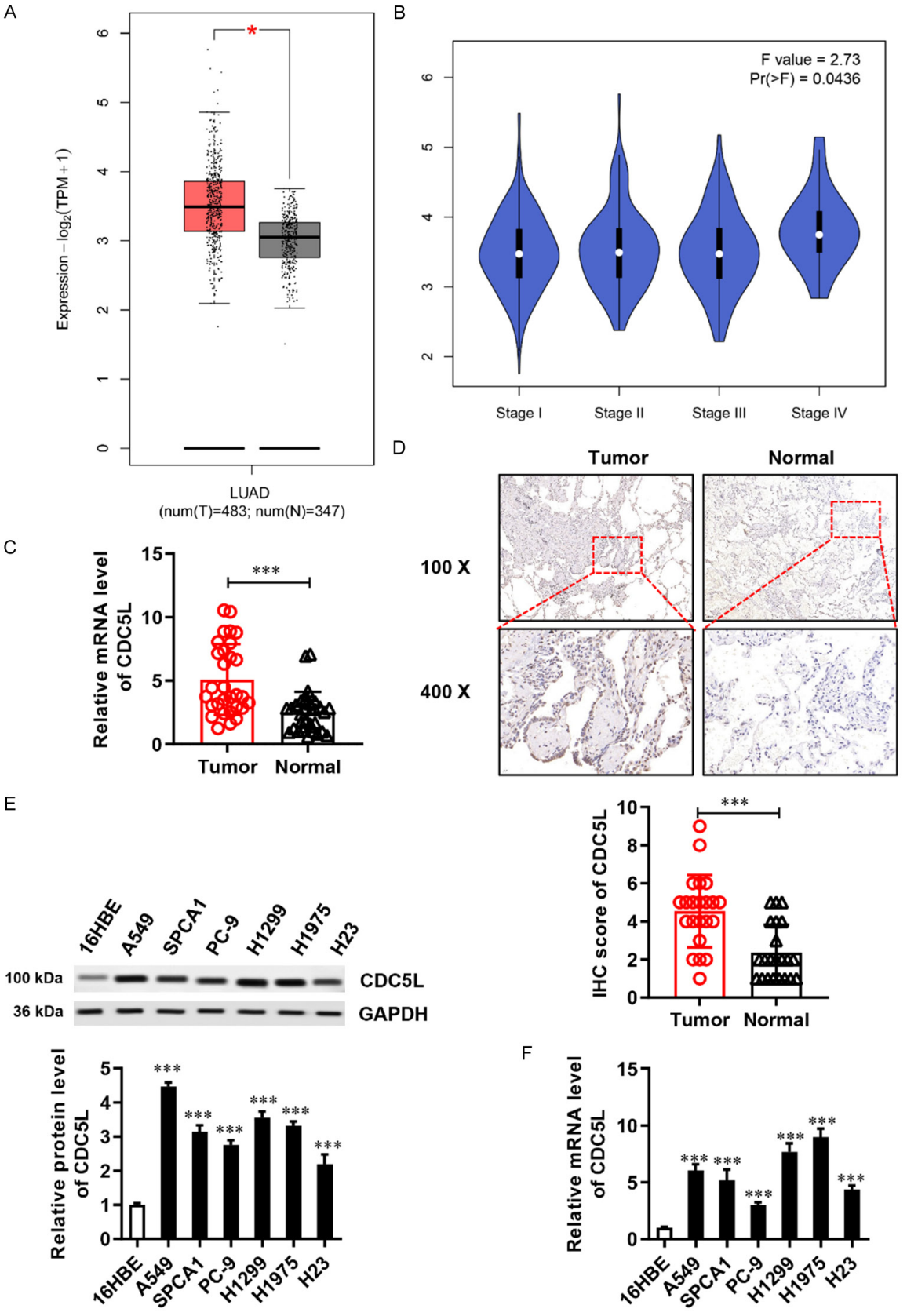

Figure 1. CDC5L was highly expressed in lung adenocarcinoma and correlated with clinicopathological characteristics. A. GEPIA database was used to analyze the expression of CDC5L in LUAD. B. Correlation between CDC5L

expression and clinical pathological characteristics. C. RT-qPCR analysis of CDC5L expression in in lung adenocarcinoma tissue (Tumor) and adjacent normal lung tissue (Normal). D. Immunohistochemical (IHC) staining for CDC5L expression is shown in lung tumor and normal tissue. E, F. Relative expression of CDC5L protein and mRNA in LUAD cell lines and normal human bronchial epithelial cell. Data are shown as the mean ± SEM. *P < 0.05, **P < 0.01, ***P < 0.001.

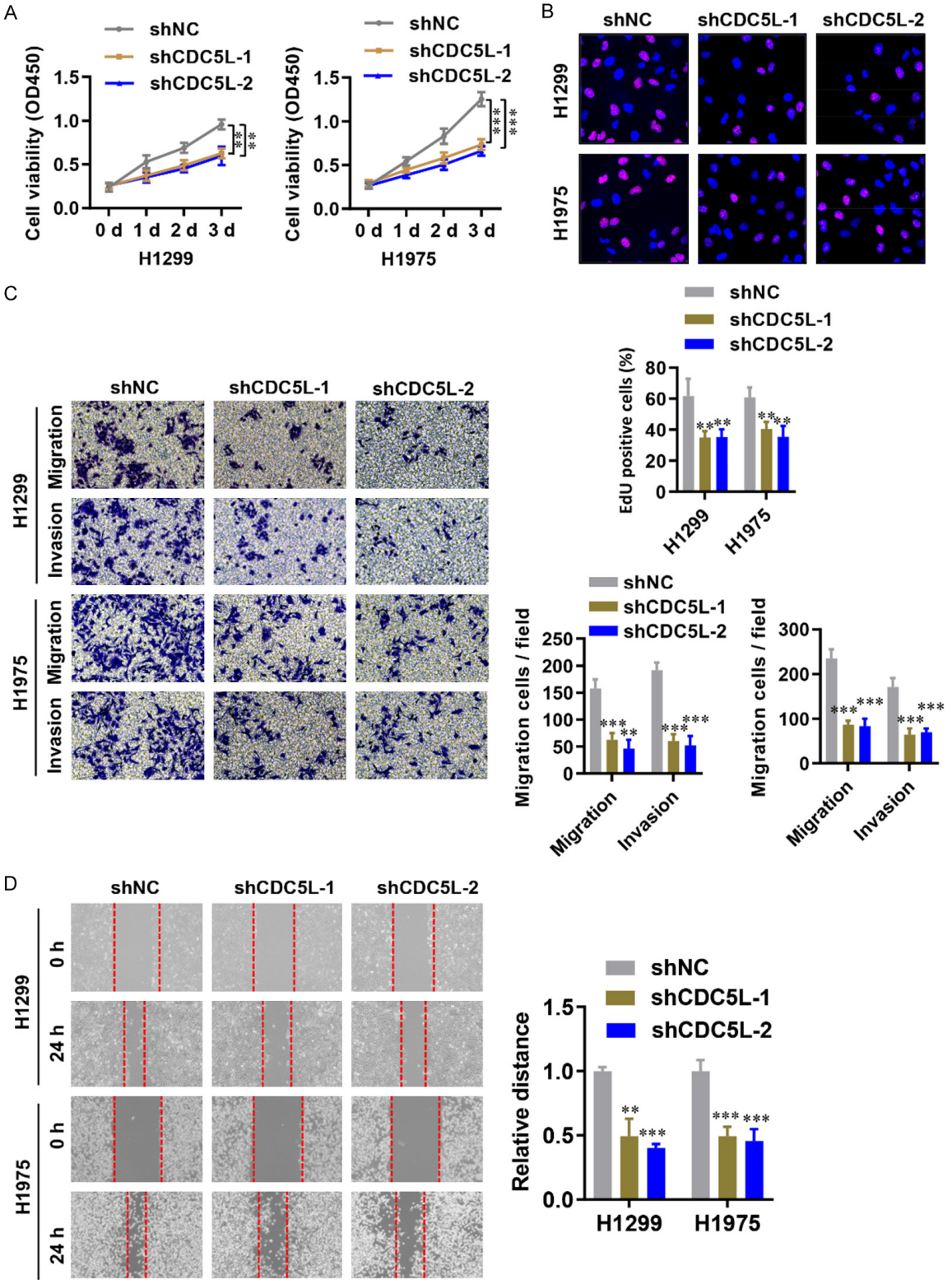

Figure 2. Knockdown of CDC5L impairs proliferation and migration of LUAD cells. A. The effect of CDC5L knockdown on H1299 and H1975 cells proliferation was detected by CCK-8 assay at the indicated time. B. Migration ability and invasion ability were determined after knockdown of CDC5L in H1299 and H1975 cells using a migration assay and a transwell assay. C. EdU-staining revealed that shCDC5L suppressed the proliferation ability of LUAD cells. D. The migration potential of H1299 and H1975 cells treated with shNC and shCDC5L were evaluated by the wound healing assay. Data are shown as the mean ± SEM. *P < 0.05, **P < 0.01, ***P < 0.001.

cells (**Figure 2B**). Additionally, EdU staining indicated that CDC5L down-regulation inhibited the proliferation capacity of LUAD cells (**Figure 2C**). Moreover, when proliferation was inhibited by 10 μg/mL mitomycin, LUAD cell migration was also reduced in the shCDC5L groups (**Figure 2D**).

To further investigate the role of CDC5L in LUAD, we transfected H1299 and H1975 cell lines with lentivirus carrying CDC5L or vector control. Western blot confirmed overexpression efficiency in both H1299 and H1975 (Figure S1B). Cells infected with CDC5L exhibited enhanced cell viability compared to the vector control (**Figure 3A**). Subsequently, we conducted colony formation assays on H1299 and H1975 cells infected with lentivirus carrying CDC5L or vector control. Our findings demonstrated that CDC5L overexpression promoted the migration of LUAD cells (**Figure 3B**). EdU staining further revealed that up-regulation of CDC5L stimulated the proliferation capacity of LUAD cells (**Figure 3C**). Furthermore, when proliferation was inhibited by 10 μg/mL mitomycin, LUAD cell migration was increased in the CDC5L up-regulation groups (**Figure 3D**). These results underscore the involvement of CDC5L in the processes of cell proliferation, migration, and invasion in LUAD cells.

CDC5L promotes LUAD growth and metastasis in vivo

To explore the oncogenic role of CDC5L *in vivo*, we utilized xenograft tumor models by transplanting LUAD cells into mice. After 30 days, the tumors were harvested and their volume and weight were measured. The results demonstrated that knockdown of CDC5L significantly suppressed tumor growth (**Figure 4A**, **4B**). This finding suggests that silencing CDC5L expression inhibits the growth of LUAD cell-derived tumors in a mouse xenograft model. Furthermore, we investigated the influence of CDC5L knockdown on the metastasis of LUAD cells *in vivo*. H1299 and H1975 cells infected with lentivirus carrying shCDC5L were injected into the tail vein of BABL/c nude mice. Hematoxylin and eosin (HE) staining was performed to evaluate the growth of LUAD xenografts in the lungs. HE staining revealed that knockdown of CDC5L inhibited the colonization of LUAD cells in the lungs (**Figure 4C**, **4D**). Overall, our findings indicate that knockdown of CDC5L effectively inhibits the metastasis and growth of LUAD cells in the lungs of nude mice compared to the control group.

CDC5L displayed its biological function via activating Wnt/β-catenin signaling pathway

To understand the underlying mechanism by which CDC5L promotes carcinogenesis in lung cancer, we conducted RNA-sequencing to identify potential downstream genes regulated by CDC5L. Our data demonstrated that knockdown of CDC5L led to a systemic decrease in the expression of genes related to the Wnt/β-catenin pathway (**Figure 5A**). Gene Set Enrichment Analysis (GSEA) further revealed a positive correlation between CDC5L expression and Wnt-activated gene signatures, suggesting that CDC5L may activate the Wnt/β-catenin signaling pathway (**Figure 5B**). To further validate the relationship between CDC5L and the Wnt/β-catenin pathway, we performed immunofluorescence (IF) staining to detect β-catenin expression in LUAD cells overexpressing or knocked down for CDC5L. The IF data demonstrated that CDC5L knockdown decreased β-catenin levels, while CDC5L overexpression increased β-catenin levels in LUAD cells (**Figure 5C**). To assess the activity of the Wnt/β-catenin pathway, we employed the TOP/FOPflash luciferase assay. Knockdown of CDC5L resulted in suppressed reporter expression, indicating reduced Wnt/β-catenin pathway activity. Conversely, upregulation of CDC5L promoted reporter expression, suggesting enhanced Wnt/β-catenin pathway activity (**Figures 5D**, S3A). We further conducted Western blot and qRT-PCR experiments to examine the impact of CDC5L on downstream genes of the Wnt/β-catenin pathway. The results showed that knockdown of CDC5L significantly downregula-

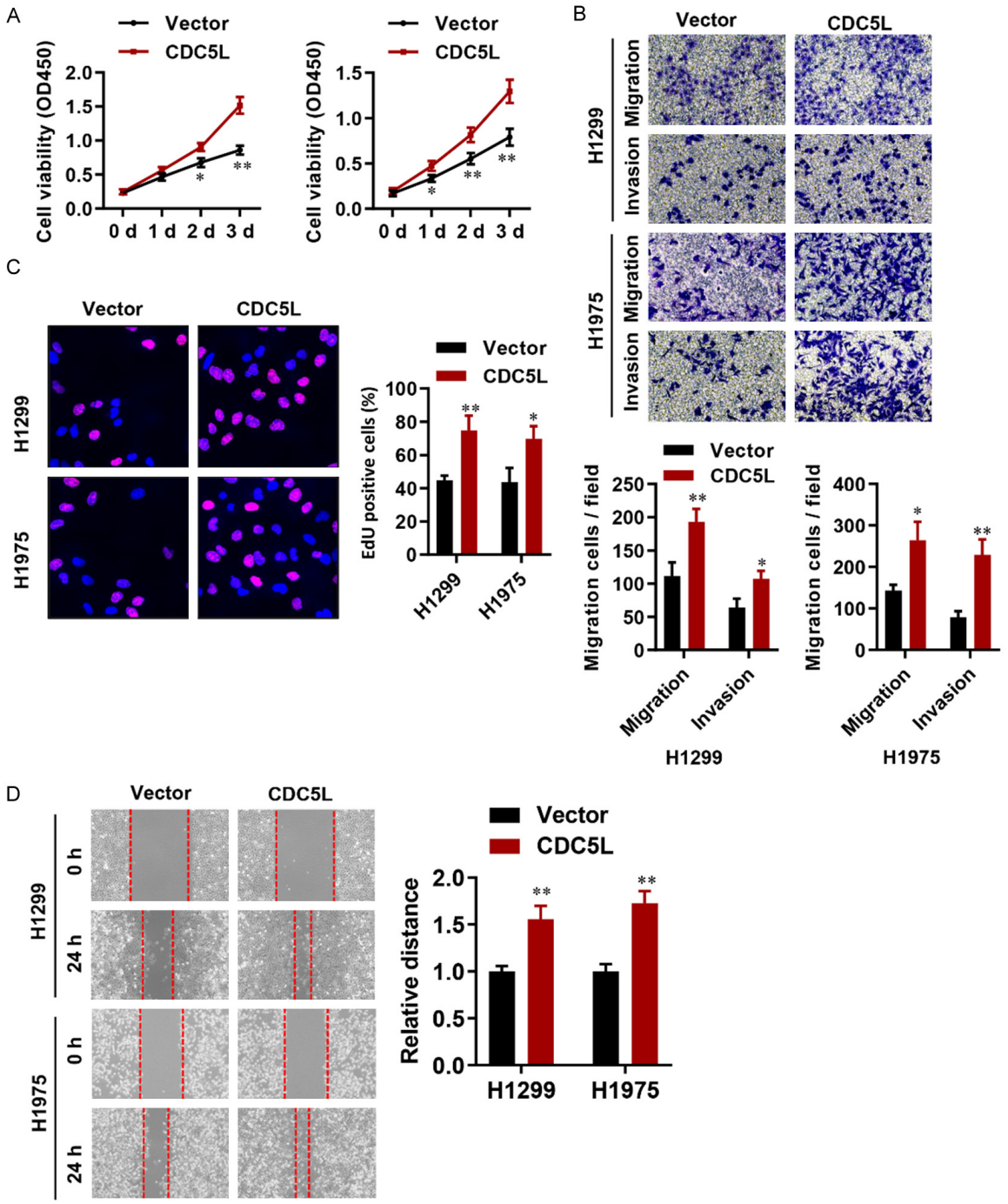

Figure 3. CDC5L overexpression promotes proliferation and migration of LUAD cells. A. The cell viability of H1299 and H1975 cells were evaluated by CCK8. B. The cell invasive ability of H1299 and H1975 cells were measured by transwell assay. C. EdU-staining revealed that CDC5L upregulation promoted the proliferation ability of LUAD cells. D. The migration potential of H1299 and H1975 cells were evaluated by the wound healing assay. Data are shown as the mean ± SEM. *P < 0.05, **P < 0.01, ***P < 0.001.

ted the expression of Axin2, c-Myc, and Cyclin D1 at both the protein and mRNA levels (**Figures 5E**, S3B). To delve deeper into the potential of CDC5L in fostering malignant characteristics in LUAD cells through the Wnt/β-catenin pathway, we subjected cells overexpressing CDC5L to treatment with the specific inhibitor of Wnt/β-catenin signaling, XAV939. The application of

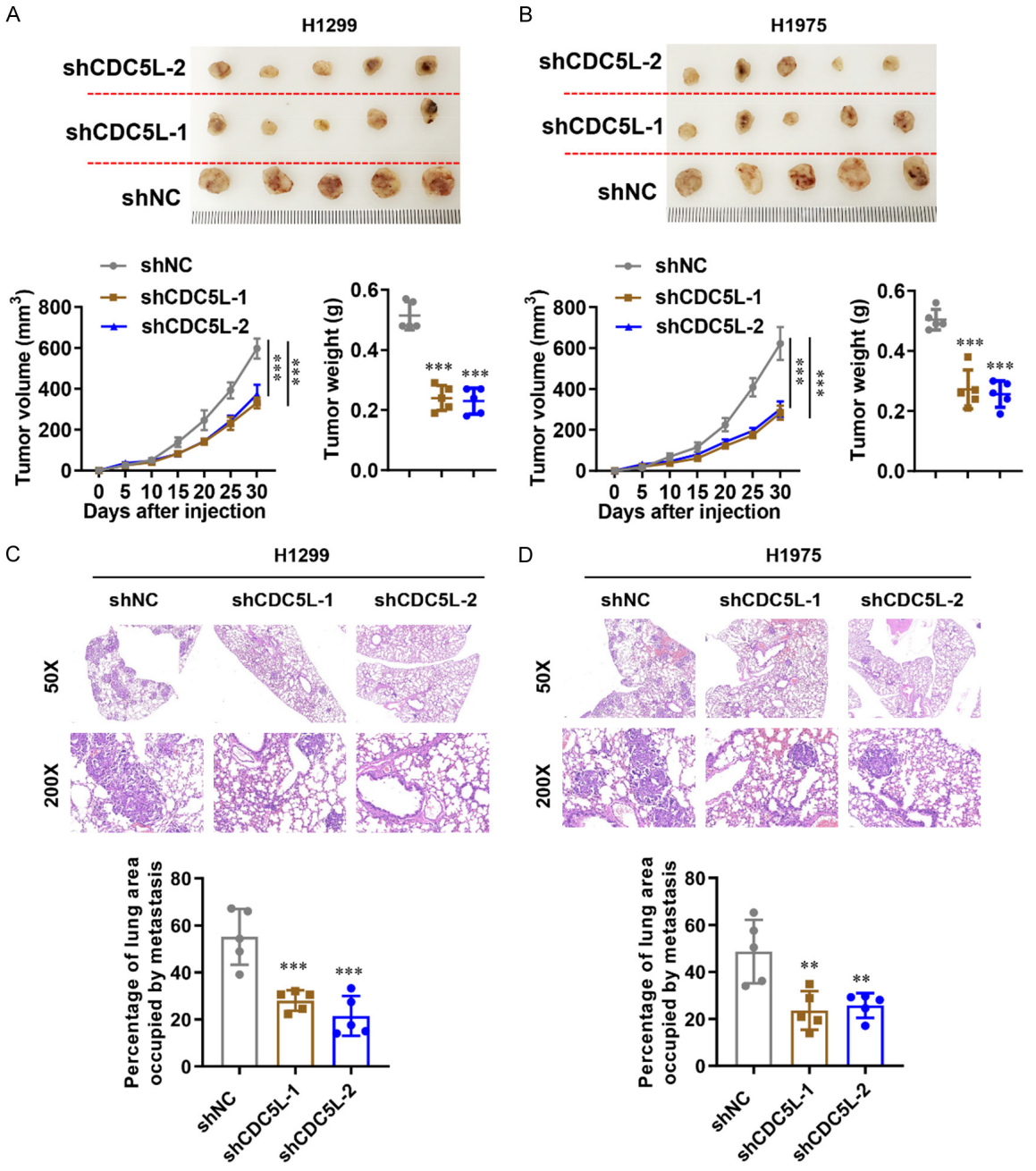

Figure 4. CDC5L knockdown inhibits growth and metastasis of LUAD cells in vivo. A, B. Quantitative analysis of the tumor volume at the indicated time (Left) and quantitative analysis of the tumor weight (Right). C, D. HE staining and quantification for lung occupancy by tumors. Data are shown as the mean ± SEM. *P < 0.05, **P < 0.01, ***P < 0.001.

XAV939 notably counteracted the proliferative effects induced by CDC5L in LUAD cells (Figure S4A, S4B). Furthermore, XAV939 mitigated the heightened migration and invasion triggered by CDC5L overexpression (Figure S4C). These findings indicate that the oncogenic role of CDC5L in lung cancer is dependent on the activation of the Wnt/β-catenin pathway.

CDC5L regulated the transcription of WNT7B in LUAD cells

It has been confirmed that CDC5L acts as a transcription factor to regulate gene expression. As shown by Animal TF DataBase, the TF binding site of CDC5L was presented (**Figure 6A**). WNT7B, one of the most important ligands

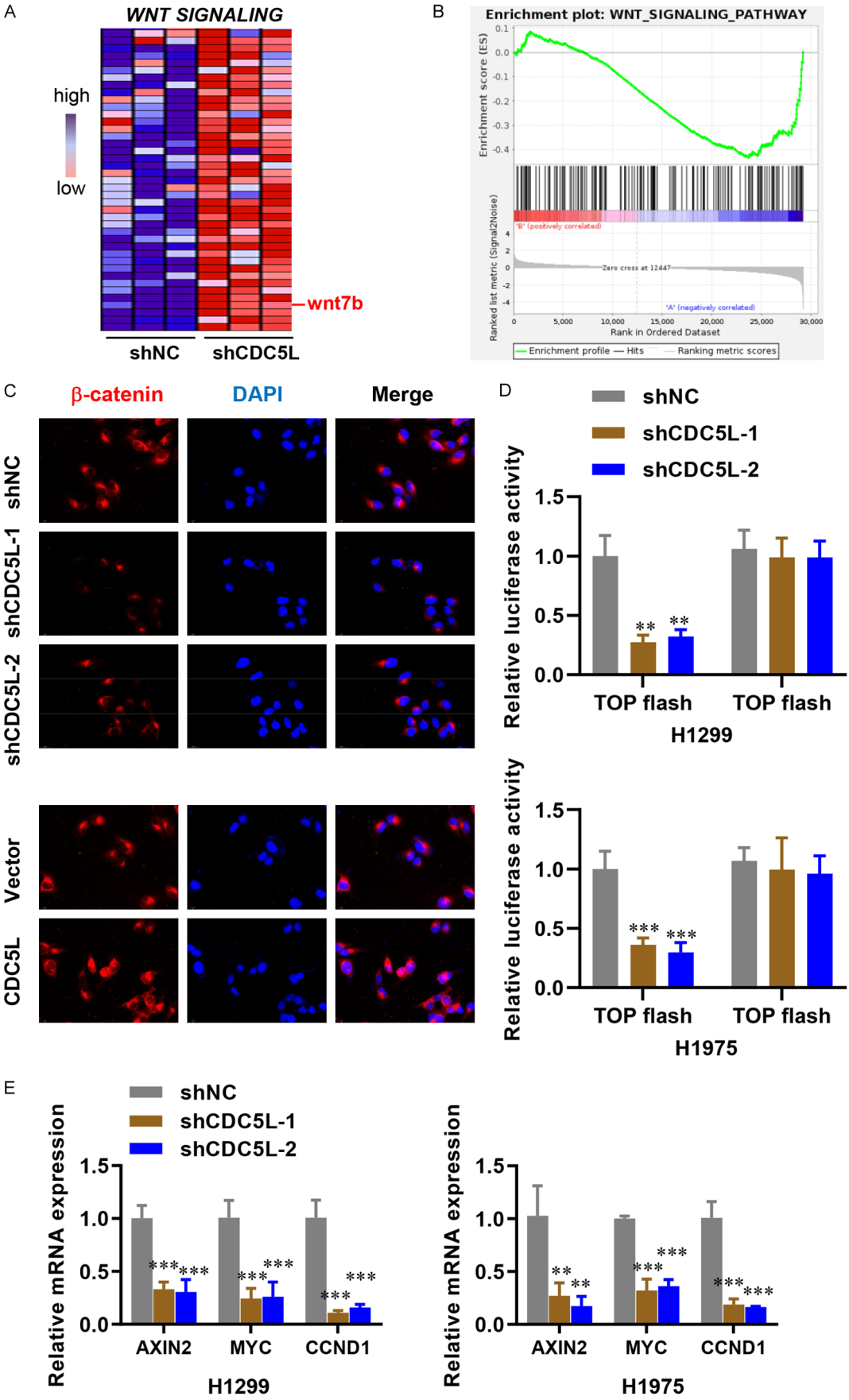
A
WNT SIGNALING
high
low
wnt7b
shNC
shCDC5L
B
Enrichment plot: WNT_SIGNALING_PATHWAY
Enrichment score (ES)
Ranked list metric (Signal2Noise)
'B' (positively correlated)
Zero cross at 12447
'A' (negatively correlated)
Rank in Ordered Dataset
Enrichment profile — Hits — Ranking metric scores
C
β-catenin
DAPI
Merge
shNC
shCDC5L-1
shCDC5L-2
Vector
CDC5L
D
shNC
shCDC5L-1
shCDC5L-2
Relative luciferase activity
TOP flash
TOP flash
H1299
H1975
E
Relative mRNA expression
AXIN2
MYC
CCND1
H1299
H1975

Figure 5. CDC5L activates the Wnt/β-catenin signaling. A. Heat map showing Z-score values of Least Squares Means for select genes associated with WNT signaling in control (CTRL) and CDC5L knockdown cells as determined using RNA-seq analysis. B. GSEA showing the positive correlations between CDC5L levels and Wnt signaling. C. Immunofluorescence staining of nuclear β-catenin expression in the indicated cells. D. Luciferase-reporter assays of TOP/FOP transcriptional activity in the indicated cells. E. Western blotting of the protein level of Wnt/β-catenin downstream genes. Data are shown as the mean ± SEM. **P < 0.01.

in canonical Wnt/β-catenin signaling pathway, has been well established in the progression of LUAD [38-40]. Predicted by hTFtarget website, CDC5L potentially targets the promoter region (-41 - -57 bp) of WNT7B (**Figure 6B**). Then we constructed luciferase reporter plasmids carrying WNT7B promoter (wild type and mutant type), and luciferase reporter assay revealed that CDC5L increased wild type but not mutant WNT7B promoter luciferase activity in both H1299 and H1975 cells (**Figure 6D**). Moreover, the results of ChIP assay suggested that CDC5L directly targeted the promoter region of WNT7B (**Figure 6C**). In H1299 and H1975 cell lines, knockdown of CDC5L suppressed the expression of WNT7B (**Figure 6E**), but overexpression of CDC5L promoted WNT7B expression (**Figure 6F**). Importantly, clinical sample data indicate that CDC5L had a positive correlation with WNT7B (R^2=0.8810, P < 0.0001) (Figure S2A). qRT-PCR indicated that WNT7B protein is highly expressed in LUAD cell lines (Figure S2B). Furthermore, we analyzed the expression of WNT7B using The Cancer Genome Atlas (TCGA) database and observed a significant increase in WNT7B expression in 59 LUAD specimens (**Figure 6G**). Kaplan-Meier curves revealed that patients with high WNT7B expression had a considerably worse prognosis compared to those with low WNT7B expression (**Figure 6H**). To further validate these findings from the TCGA database, we examined the expression of WNT7B in patient samples. Our results demonstrated a significantly higher protein level of WNT7B in LUAD tissue compared to normal lung tissues (**Figure 6I**). These findings indicated that CDC5L controlled the activity of Wnt/β-catenin signaling pathway via transcriptional regulating WNT7B.

WNT7B is indispensable for the CDC5L-mediated activation of Wnt/β-catenin signaling and LUAD progression

Based on the correlation between CDC5L and WNT7B, we investigated whether WNT7B serves as a key molecule in the CDC5L-mediated regulation of LUAD development. The positive effects of CDC5L on LUAD cell viability was almost completely abolished after the knockdown of WNT7B expression (**Figure 7A**). EdU-staining also revealed that WNT7B knockdown significantly abolished the pro-proliferation ability of CDC5L on LUAD cells (**Figure 7B**). Furthermore, we performed transwell and wound healing assays to evaluate the impact of WNT7B knockdown on cell migration and invasion, and observed that the suppression of cell migration and invasion caused by CDC5L downregulation was nearly completely abolished by WNT7B knockdown (**Figure 7C**). Furthermore, in the xenograft mice model, the overexpression of CDC5L significantly promoted tumor growth, and this effect was partially reversed by silencing WNT7B in LUAD cells (**Figure 7D**, **7E**). Additionally, in the in vivo metastasis assay, the heightened metastatic activity resulting from CDC5L overexpression was partially reversed by WNT7B knockdown (**Figure 7F**). Collectively, these findings suggest that CDC5L promotes LUAD cell proliferation and metastasis by activating the Wnt/β-catenin pathway through the regulation of WNT7B expression.

m^6A modification contributes to the upregulation of CDC5L in LUAD

To investigate the impact of m^6A alteration on CDC5L elevation, we examined multiple m^6A sites within the CDC5L transcript using the SRAMP prediction server (**Figure 8A**). Subsequently, an m^6A RIP assay demonstrated increased m^6A levels in H1299 and H1975 cells compared to normal bronchial epithelial cells (16HBE) (**Figure 8B**), suggesting a potential role for m^6A in upregulating CDC5L. Notably, a positive correlation between METTL14 and CDC5L levels was observed in LUAD tissues from the TCGA dataset (**Figure 8C**), supporting the regulatory role of METTL14 on CDC5L. Given METTL14's dysregulation in human cancers and its involvement in the N6-methyltransferase complex, we examined its impact on the m^6A modification of CDC5L. Silencing METTL14 using siRNA in LUAD cells resulted in a significant reduction in CDC5L m^6A levels

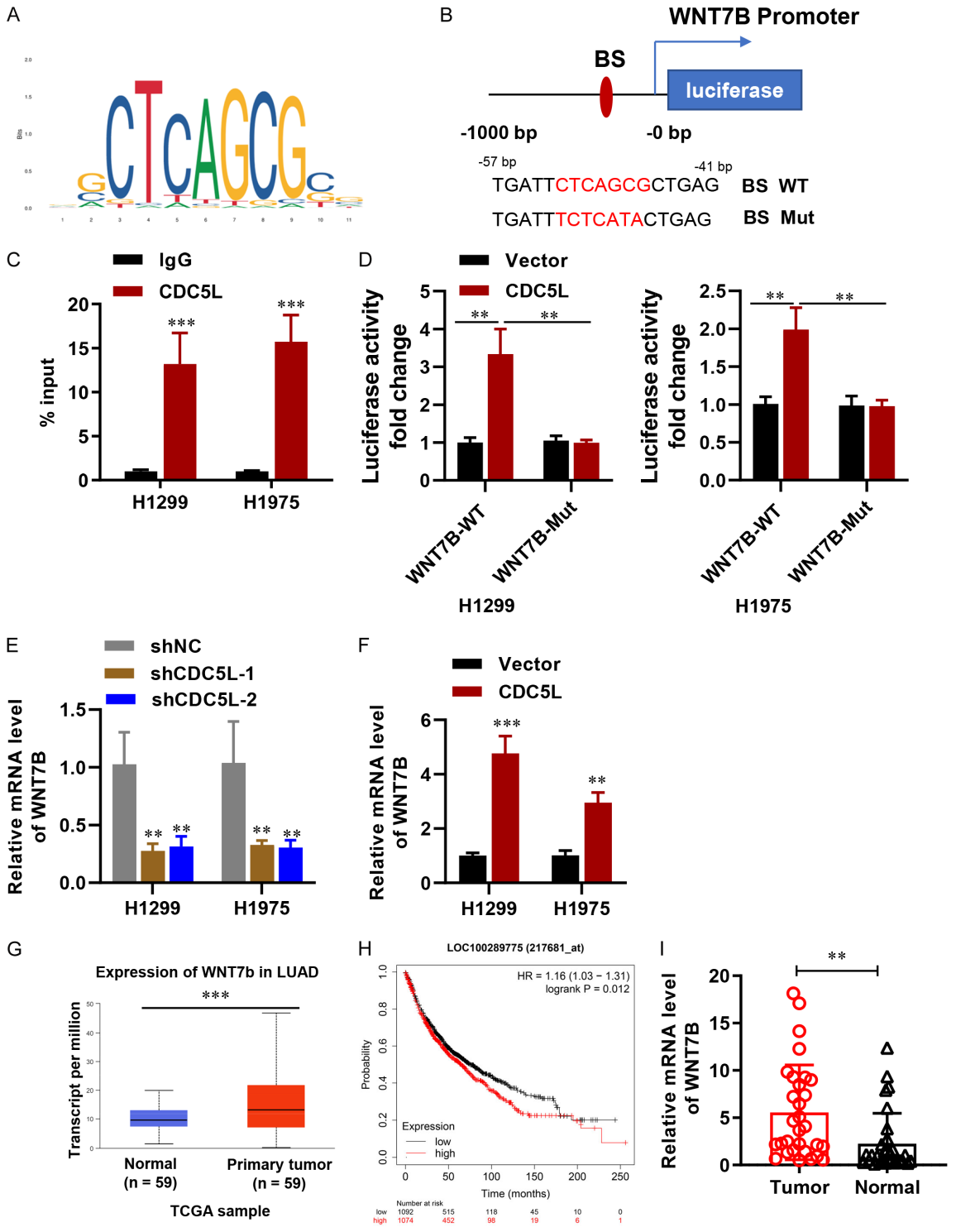

Figure 6. CDC5L regulated WNT7B transcription by directly binding to its promoter region. A. The TF binding site of CDC5L was shown by Animal TF DataBase. B. Predicted by hTFtarget website, CDC5L directly binds to the promoter region (41-57 bp) of WNT7B. C. In ChIP assay, CDC5L antibody recruited WNT7B promoter DNA fragment. The IgG antibody and control primer were used as negative controls. D. Ectopic expression of CDC5L increased wild type but not mutant WNT7B promoter luciferase activity. E. The expression of WNT7B was decreased by knockdown of CDC5L. F. The expression of WNT7B was increased by upregulation of CDC5L. G. WNT7B mRNA expression in The Cancer Genome Atlas (TCGA) cohort. H. Kaplan-Meier plotter database showed that high WNT7B levels were significantly ($P < 0.05$) associated with poor overall survival in patients with LUAD. I. RT-qPCR analysis of WNT7B expression in in lung adenocarcinoma tissue (Tumor) and adjacent normal lung tissue (Normal). Data are shown as the mean ± SEM. *$P < 0.05$, **$P < 0.01$, ***$P < 0.001$.

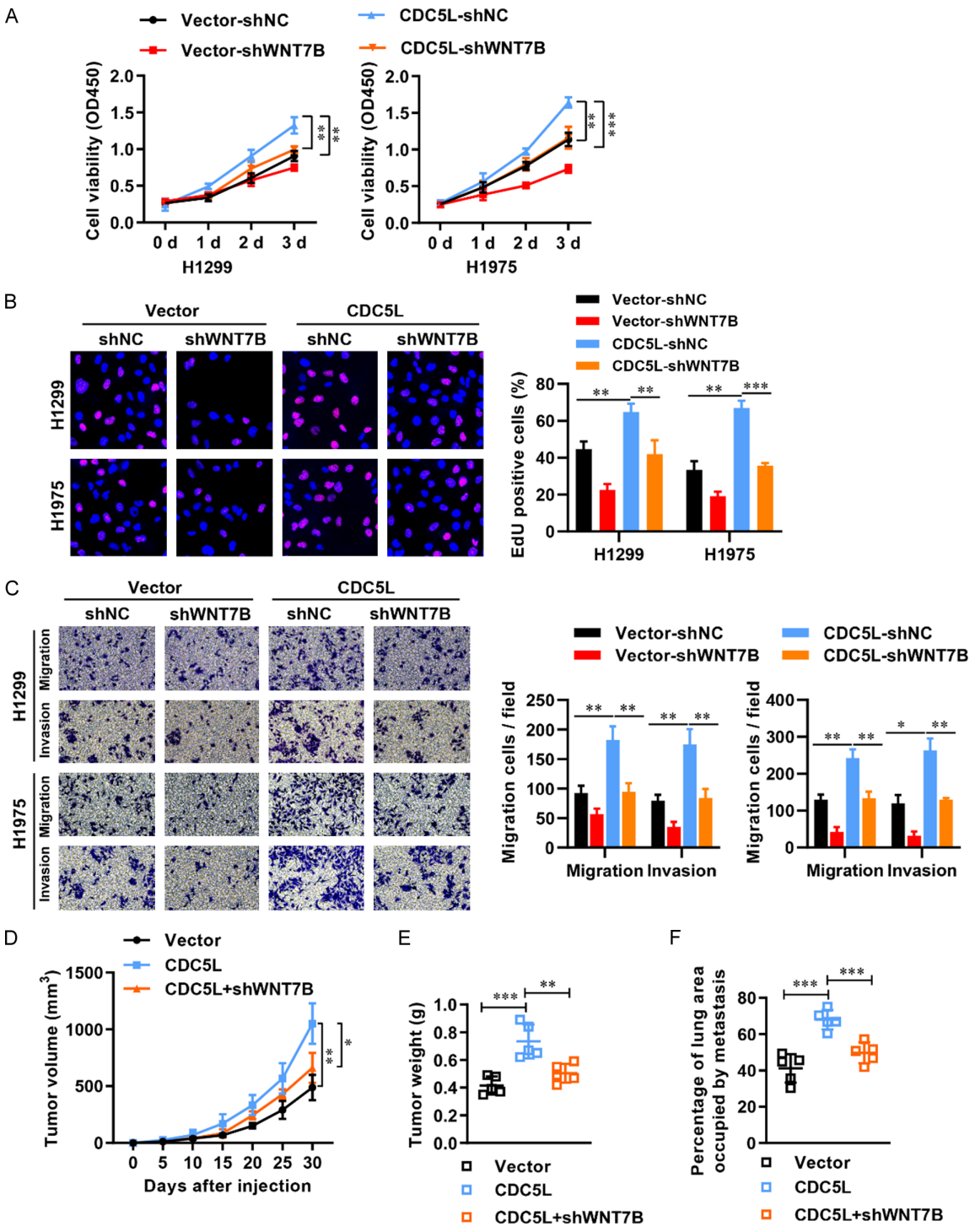

Figure 7. WNT7B is indispensable for the CDC5L-mediated activation of Wnt/β-catenin signaling and LUAD progression. (A) The positive effects of CDC5L on LUAD cell viability was almost completely abolished after the knockdown of WNT7B expression. (B) EdU-staining also revealed that WNT7B knockdown significantly abolished the pro-proliferation ability of CDC5L on LUAD cells. (C) Transwell assay and wound healing assay for cell migration and invasion of LUAD cells. (D, E) Quantitative analysis of the tumor volume at the indicated time (D) and quantitative analysis of the tumor weight (E). (F) The percentage of lung areas occupied by tumors is quantified. Data are shown as the mean ± SEM. *P < 0.05, **P < 0.01, ***P < 0.001.

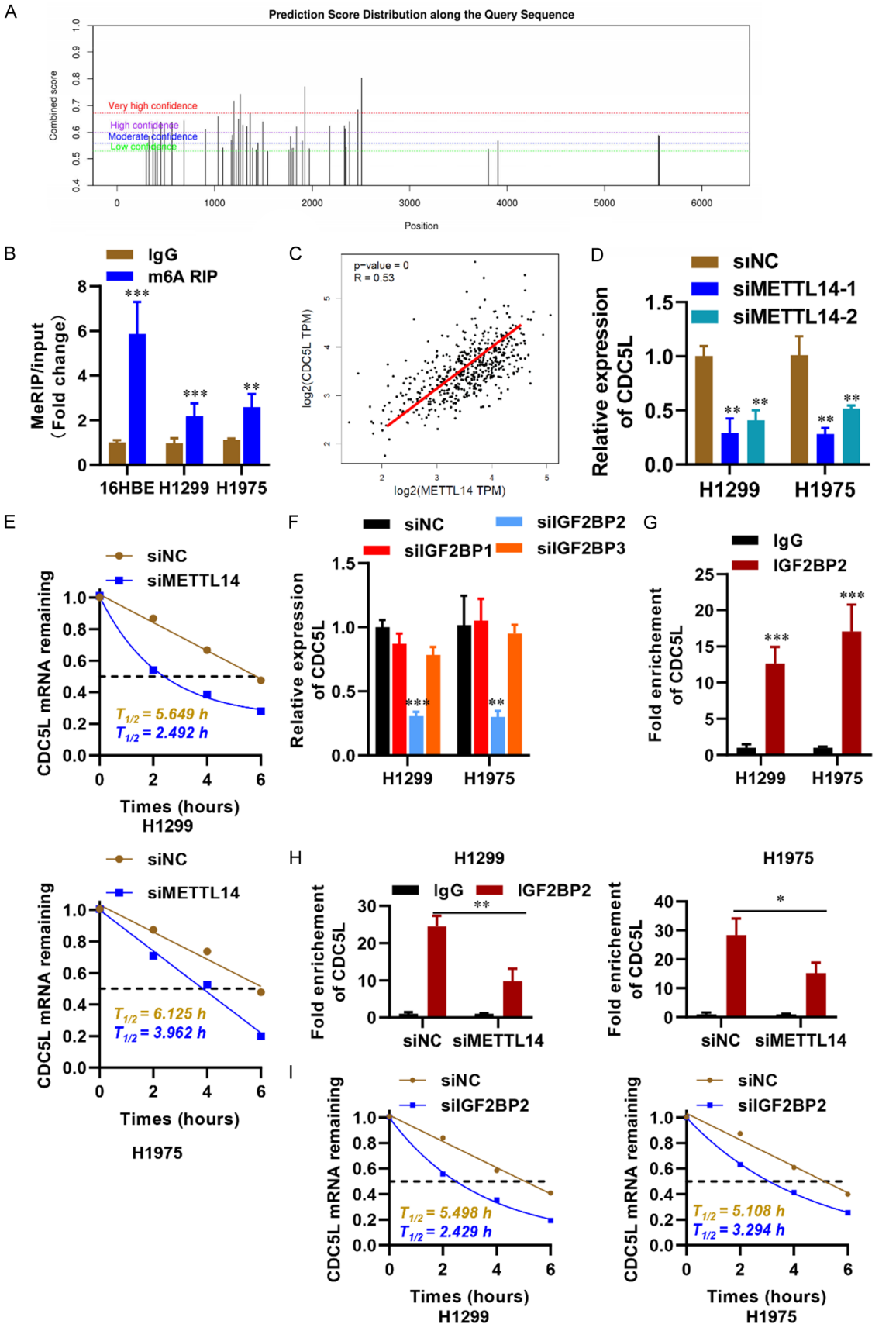
A
Prediction Score Distribution along the Query Sequence
Combined score
Very high confidence
High confidence
Moderate confidence
Low confidence
Position
B
IgG
m6A RIP
MeRIP/input (Fold change)
16HBE H1299 H1975
C
p-value = 0
R = 0.53
log2(CDC5L TPM)
log2(METTL14 TPM)
D
siNC
siMETTL14-1
siMETTL14-2
Relative expression of CDC5L
H1299 H1975
E
siNC
siMETTL14
CDC5L mRNA remaining
T1/2 = 5.649 h
T1/2 = 2.492 h
Times (hours)
H1299
T1/2 = 6.125 h
T1/2 = 3.962 h
H1975
F
siNC
siIGF2BP1
siIGF2BP2
siIGF2BP3
Relative expression of CDC5L
H1299 H1975
G
IgG
IGF2BP2
Fold enrichement of CDC5L
H1299 H1975
H
H1299
H1975
IgG
IGF2BP2
Fold enrichement of CDC5L
siNC siMETTL14
I
siNC
siIGF2BP2
CDC5L mRNA remaining
T1/2 = 5.498 h
T1/2 = 2.429 h
Times (hours)
H1299
T1/2 = 5.108 h
T1/2 = 3.294 h
H1975

Figure 8. The upregulation of CDC5L in LUAD is attribute to m^{6}A modification. A. Prediction of multiple m^{6}A sites in the CDC5L transcript using the SRAMP prediction server. B. m^{6}A RIP-qPCR analysis of CDC5L expression in 16HBE, H1299, and H1975 cells. C. Correlation analysis showing the correlation between METTL14 and CDC5L in the TCGA dataset. D. qPCR analysis of CDC5L expression with METTL14 knockdown. E. Examination of CDC5L mRNA half-lives in METTL14 knockdown LUAD cells. F. Cells were knocked down of IGF2BP1/2/3 by siRNA. The expressions of TRIB3 were analyzed by qPCR. G. RIP analysis indicating enrichment of CDC5L by IGF2BP2. H. LUAD cells were transfected with or without specific siRNA for METTL14. RIP analyses were performed with an anti-IGF2BP2 antibody. I. Examination of CDC5L mRNA half-lives in the LUAD cells with IGF2BP2 knockdown. Data are shown as the mean ± SEM. *P < 0.05, **P < 0.01, ***P < 0.001.

(data not shown) and decreased CDC5L expression (**Figure 8D**). Further experiments were conducted to explore the specific mechanism underlying the m^{6}A-induced upregulation of CDC5L in LUAD cells. Evaluating the effect of reducing METTL14 on CDC5L stability revealed a noticeable decrease in CDC5L half-life in LUAD cells treated with METTL14 siRNA (**Figure 8E**), indicating that METTL14 regulates CDC5L expression by influencing its stability.

To explore the mechanisms governing CDC5L stability, we investigated potential proteins that could act as m^{6}A readers to detect methylated CDC5L. The regulation of CDC5L by m^{6}A modification depends on the recognition of methylated CDC5L. Previous studies have suggested that IGF2BP family proteins serve as m^{6}A 'readers' to enhance mRNA stability [41, 42]. To further understand the complete modification mechanism of METTL14-CDC5L in LUAD, we used siRNA transfection to knock down IGF2BP1, 2, and 3 in tumor cells (Figure S5). Our results revealed that specifically silencing IGF2BP2, not IGF2BP1 or IGF2BP3, significantly affected the expression levels of CDC5L (**Figure 8F**). Subsequent analysis using RIP showed a substantial enrichment of CDC5L by the IGF2BP2 protein (**Figure 8G**), which was diminished upon METTL14 depletion (**Figure 8H**), indicating that METTL14-induced m^{6}A modification influenced the recognition and binding of methylated CDC5L by IGF2BP2. Moreover, silencing IGF2BP2 in LUAD cells led to a notable acceleration in the decay rate of CDC5L (**Figure 8I**), consistent with the results observed when inhibiting METTL14. These collective findings suggest that IGF2BP2 acts as an m^{6}A reader for CDC5L. Overall, our data strongly support the role of m^{6}A alteration in the upregulation of CDC5L in LUAD cells.

Discussion

CDC5L is a protein involved in regulating the G2/M transition of the cell cycle, as well as participating in pre-mRNA splicing and DNA damage repair. Recently, it has been identified as a potential oncogene in osteosarcoma and cervical tumors [11, 15, 43]. However, the role of CDC5L in the progression of lung adenocarcinoma (LUAD) remains unclear. This study aimed to explore the expression and clinical implications of CDC5L in LUAD. Our findings revealed elevated CDC5L expression in LUAD tissues, significantly correlating with TNM staging. Notably, high CDC5L levels independently predicted poorer survival among LUAD patients. Furthermore, silencing CDC5L suppressed proliferation and induced apoptosis in LUAD cells. Additionally, increased CDC5L expression correlated with worse overall survival and advanced clinical stage in LUAD patients. Mechanistically, CDC5L activated the Wnt/β-catenin pathway by transcriptionally upregulating WNT7B, thereby promoting LUAD progression. These results provide compelling evidence supporting CDC5L as a promising therapeutic target in LUAD. Targeting CDC5L holds potential to inhibit LUAD growth and enhance patient outcomes.

The Wnt signaling pathway plays a significant role in the development and progression of various cancers, including LUAD [44-47]. In LUAD, aberrant activation of the Wnt pathway has been observed and is associated with tumor growth, metastasis, and poor prognosis [30-33]. In our study, we found that CDC5L activates the Wnt/β-catenin signaling pathway in LUAD. This finding further highlights the relevance of the Wnt pathway in LUAD progression. Activation of the Wnt pathway leads to the stabilization and nuclear translocation of β-catenin, resulting in the transcriptional activation of target genes involved in cell proliferation, survival, and invasion [27-29]. The dysregulation of the Wnt pathway in LUAD can occur through various mechanisms. Mutations in key components of the pathway, such as APC, β-catenin, or Axin, can lead to constitutive activation of the pathway. Additionally, alterations

in upstream regulators or downstream effectors can also contribute to Wnt pathway activation [48-52]. Targeting the Wnt signaling pathway in LUAD holds promise as a therapeutic strategy. Various approaches have been explored, including inhibition of Wnt ligands, disruption of the interaction between Wnt ligands and receptors, and inhibition of β-catenin transcriptional activity. These approaches aim to inhibit Wnt pathway activation and subsequent tumor growth and metastasis. Understanding the interaction between CDC5L and the Wnt pathway offers insights into the mechanisms driving LUAD progression. Targeting CDC5L could potentially modulate the Wnt pathway, thereby impeding LUAD development and enhancing patient outcomes. Further research is essential to elucidate the precise molecular mechanisms underlying Wnt pathway dysregulation in LUAD and to explore innovative therapeutic strategies aimed at this pathway.

m^6A modification is the predominant RNA modification and exerts influence on various stages of the RNA life cycle, such as processing, translocation, degradation, and translation. Our results highlight the importance of m^6A modification in CDC5L upregulation in LUAD cells, revealing a potential novel regulatory mechanism for CDC5L expression. Overall, our comprehensive findings provide compelling evidence for the crucial role of CDC5L in LUAD. Its upregulation in tumor tissues, association with aggressive clinicopathological features, and independent prognostic value underscore CDC5L as a promising therapeutic target in LUAD. Targeting CDC5L in LUAD treatment offers significant advantages due to its high expression in LUAD tissues, positively correlating with clinicopathological features such as pathology grade and proliferation potential. Elevated CDC5L expression also acts as an independent prognostic factor for poorer overall survival in LUAD patients. Inhibiting CDC5L suppresses LUAD cell proliferation, hinders tumor growth, and potentially disrupts the critical Wnt/β-catenin pathway involved in cancer progression. This comprehensive approach holds promise for improving patient outcomes by addressing multiple facets of LUAD development and progression.

Acknowledgements

This study was supported by Young Scientific Research Program, Fujian provincial health technology project (Grant number: 2020QNA-033), Startup Fund for scientific research, Fujian Medical University (Grant number: 2021QH1028), Startup Fund for scientific research, Fujian Medical University (Grant number: 2019QH1051) and Joint Funds for the innovation of science and technology, Fujian province (Grant number: 2021Y9077).

Disclosure of conflict of interest

None.

Address correspondence to: Weidong Wu, Department of Thoracic Surgery, Fujian Medical University Union Hospital, No. 29 Xinquan Road, Fuzhou 350001, Fujian, China. E-mail: wuweidong@fjmu.edu.cn

References

[1] Bray F, Ferlay J, Soerjomataram I, Siegel RL, Torre LA and Jemal A. Global cancer statistics 2018: GLOBOCAN estimates of incidence and mortality worldwide for 36 cancers in 185 countries. CA Cancer J Clin 2018; 68: 394-424.

[2] Siegel RL, Miller KD and Jemal A. Cancer statistics, 2018. CA Cancer J Clin 2018; 68: 7-30.

[3] Duruisseaux M and Esteller M. Lung cancer epigenetics: from knowledge to applications. Semin Cancer Biol 2018; 51: 116-128.

[4] Hirsch FR, Scagliotti GV, Mulshine JL, Kwon R, Curran WJ Jr, Wu YL and Paz-Ares L. Lung cancer: current therapies and new targeted treatments. Lancet 2017; 389: 299-311.

[5] Chen Z, Fillmore CM, Hammerman PS, Kim CF and Wong KK. Non-small-cell lung cancers: a heterogeneous set of diseases. Nat Rev Cancer 2014; 14: 535-546.

[6] Bernstein HS and Coughlin SR. A mammalian homolog of fission yeast Cdc5 regulates G2 progression and mitotic entry. J Biol Chem 1998; 273: 4666-4671.

[7] Nasmyth K and Nurse P. Cell division cycle mutants altered in DNA replication and mitosis in the fission yeast Schizosaccharomyces pombe. Mol Gen Genet 1981; 182: 119-124.

[8] Zhang N, Kaur R, Akhter S and Legerski RJ. Cdc5L interacts with ATR and is required for the S-phase cell-cycle checkpoint. EMBO Rep 2009; 10: 1029-1035.

[9] Lu XY, Lu Y, Zhao YJ, Jaeweon K, Kang J, Xiao-Nan L, Ge G, Meyer R, Perlaky L, Hicks J, Chintagumpala M, Cai WW, Ladanyi M, Gorlick R, Lau CC, Pati D, Sheldon M and Rao PH. Cell cycle regulator gene CDC5L, a potential target for 6p12-p21 amplicon in osteosarcoma. Mol Cancer Res 2008; 6: 937-946.

[10] Burns CG, Ohi R, Krainer AR and Gould KL. Evidence that Myb-related CDC5 proteins are required for pre-mRNA splicing. Proc Natl Acad Sci U S A 1999; 96: 13789-13794.
[11] Mu R, Wang YB, Wu M, Yang Y, Song W, Li T, Zhang WN, Tan B, Li AL, Wang N, Xia Q, Gong WL, Wang CG, Zhou T, Guo N, Sang ZH and Li HY. Depletion of pre-mRNA splicing factor Cdc5L inhibits mitotic progression and triggers mitotic catastrophe. Cell Death Dis 2014; 5: e1151.
[12] Li J, Zhang N, Zhang R, Sun L, Yu W, Guo W, Gao Y, Li M, Liu W, Liang P, Deng W and Cui X. CDC5L promotes hTERT expression and colorectal tumor growth. Cell Physiol Biochem 2017; 41: 2475-2488.
[13] Bonczek O, Wang L, Gnanasundram SV, Chen S, Haronikova L, Zavadil-Kokas F and Vojtesek B. DNA and RNA binding proteins: from motifs to roles in cancer. Int J Mol Sci 2022; 23: 9329.
[14] Fragkiadaki P, Renieri E, Kalliantasi K, Kouvidi E, Apalaki E, Vakonaki E, Mamoulakis C, Spandidos DA and Tsatsakis A. Tauelomerase inhibitors and activators in aging and cancer: a systematic review. Mol Med Rep 2022; 25: 158.
[15] Chen W, Zhang L, Wang Y, Sun J, Wang D, Fan S, Ban N, Zhu J, Ji B and Wang Y. Expression of CDC5L is associated with tumor progression in gliomas. Tumour Biol 2016; 37: 4093-4103.
[16] Zhang Z, Mao W, Wang L, Liu M, Zhang W, Wu Y, Zhang J, Mao S, Geng J and Yao X. Depletion of CDC5L inhibits bladder cancer tumorigenesis. J Cancer 2020; 11: 353-363.
[17] Neubauer G, King A, Rappsilber J, Calvio C, Watson M, Ajuh P, Sleeman J, Lamond A and Mann M. Mass spectrometry and EST-database searching allows characterization of the multi-protein spliceosome complex. Nat Genet 1998; 20: 46-50.
[18] Liu H, Lyu H, Jiang G, Chen D, Ruan S, Liu S, Zhou L, Yang M, Zeng S, He Z, Wang H, Li H, Zheng G and Liu B. ALKBH5-mediated m6A demethylation of GLUT4 mRNA promotes glycolysis and resistance to HER2-targeted therapy in breast cancer. Cancer Res 2022; 82: 3974-3986.
[19] Xu Y, Song M, Hong Z, Chen W, Zhang Q, Zhou J, Yang C, He Z, Yu J, Peng X, Zhu Q, Li S, Ji K, Liu M and Zuo Q. The N6-methyladenosine METTL3 regulates tumorigenesis and glycolysis by mediating m6A methylation of the tumor suppressor LATS1 in breast cancer. J Exp Clin Cancer Res 2023; 42: 10.
[20] Roundtree IA, Evans ME, Pan T and He C. Dynamic RNA modifications in gene expression regulation. Cell 2017; 169: 1187-1200.
[21] Haruehanroengra P, Zheng YY, Zhou Y, Huang Y and Sheng J. RNA modifications and cancer. RNA Biol 2020; 17: 1560-1575.
[22] Tuncel G and Kalkan R. Importance of m N(6)-methyladenosine (m(6)A) RNA modification in cancer. Med Oncol 2019; 36: 36.
[23] Wu L, Wu D, Ning J, Liu W and Zhang D. Changes of N6-methyladenosine modulators promote breast cancer progression. BMC Cancer 2019; 19: 326.
[24] Miyake K, Costa Cruz PH, Nagatomo I, Kato Y, Motooka D, Satoh S, Adachi Y, Takeda Y, Kawahara Y and Kumanogoh A. A cancer-associated METTL14 mutation induces aberrant m6A modification, affecting tumor growth. Cell Rep 2023; 42: 112688.
[25] Hasan H, Afzal M, Castresana JS and Shahi MH. A comprehensive review of miRNAs and their epigenetic effects in glioblastoma. Cells 2023; 12: 1578.
[26] Hashemi M, Daneii P, Zandieh MA, Raesi R, Zahmatkesh N, Bayat M, Abuelrub A, Khazaei Koohpar Z, Aref AR, Zarrabi A, Rashidi M, Salimimoghadam S, Entezari M, Taheriazam A and Khorrami R. Non-coding RNA-mediated N6-methyladenosine (m(6)A) deposition: a pivotal regulator of cancer, impacting key signaling pathways in carcinogenesis and therapy response. Noncoding RNA Res 2023; 9: 84-104.
[27] Nusse R and Clevers H. Wnt/beta-catenin signaling, disease, and emerging therapeutic modalities. Cell 2017; 169: 985-999.
[28] He S and Tang S. WNT/beta-catenin signaling in the development of liver cancers. Biomed Pharmacother 2020; 132: 110851.
[29] Zhao H, Ming T, Tang S, Ren S, Yang H, Liu M, Tao Q and Xu H. Wnt signaling in colorectal cancer: pathogenic role and therapeutic target. Mol Cancer 2022; 21: 144.
[30] Stewart DJ. Wnt signaling pathway in non-small cell lung cancer. J Natl Cancer Inst 2014; 106: djt356.
[31] Wu Q, Li R, Wang QX, Zhang MY, Liu TT and Qu YQ. Junctional adhesion molecule-like protein promotes tumor progression via the Wnt/beta-catenin signaling pathway in lung adenocarcinoma. J Transl Med 2022; 20: 260.
[32] Wan H, Lin T, Shan M, Lu J and Guo Z. LINC00491 facilitates tumor progression of lung adenocarcinoma via Wnt/beta-catenin-signaling pathway by regulating MTSS1 ubiquitination. Cells 2022; 11: 3737.
[33] Zhou HM and Zhao LM. Wnt signaling pathway-derived score for predicting therapeutic resistance and tumor microenvironment in lung adenocarcinoma. Front Pharmacol 2023; 13: 1091018.

[34] Wu Q, Wang J, Tan WLW, Jiang Y, Wang S, Li Q, Yu X, Tan J, Liu S, Zhang P, Tiang Z, Chen Z, Foo RS and Yang HT. Extracellular vesicles from human embryonic stem cell-derived cardiovascular progenitor cells promote cardiac infarct healing through reducing cardiomyocyte death and promoting angiogenesis. Cell Death Dis 2020; 11: 354.
[35] Glenn HL, Messner J and Meldrum DR. A simple non-perturbing cell migration assay insensitive to proliferation effects. Sci Rep 2016; 6: 31694.
[36] Simpson MJ, Treloar KK, Binder BJ, Haridas P, Manton KJ, Leavesley DI, McElwain DL and Baker RE. Quantifying the roles of cell motility and cell proliferation in a circular barrier assay. J R Soc Interface 2013; 10: 20130007.
[37] Bi W, Wang J, Jiang Y, Li Q, Wang S, Liu M, Liu Q, Li F, Paul C, Wang Y and Yang HT. Neurotrophin-3 contributes to benefits of human embryonic stem cell-derived cardiovascular progenitor cells against reperfused myocardial infarction. Stem Cells Transl Med 2021; 10: 756-772.
[38] Tammela T, Sanchez-Rivera FJ, Cetinbas NM, Wu K, Joshi NS, Helenius K, Park Y, Azimi R, Kerper NR, Wesselhoeft RA, Gu X, Schmidt L, Cornwall-Brady M, Yilmaz OH, Xue W, Katajisto P, Bhutkar A and Jacks T. A Wnt-producing niche drives proliferative potential and progression in lung adenocarcinoma. Nature 2017; 545: 355-359.
[39] Ning J, Wang F, Bu J, Zhu K and Liu W. Downregulated m6A reader FTO destabilizes PHF1 that triggers enhanced stemness capacity and tumor progression in lung adenocarcinoma. Cell Death Discov 2022; 8: 354.
[40] Zheng Q, Min S and Zhou Q. Identification of potential diagnostic and prognostic biomarkers for LUAD based on TCGA and GEO databases. Biosci Rep 2021; 41: BSR20204370.
[41] Huang H, Weng H, Sun W, Qin X, Shi H, Wu H, Zhao BS, Mesquita A, Liu C, Yuan CL, Hu YC, Huttelmaier S, Skibbe JR, Su R, Deng X, Dong L, Sun M, Li C, Nachtergaele S, Wang Y, Hu C, Ferchen K, Greis KD, Jiang X, Wei M, Qu L, Guan JL, He C, Yang J and Chen J. Recognition of RNA N(6)-methyladenosine by IGF2BP proteins enhances mRNA stability and translation. Nat Cell Biol 2018; 20: 285-295.
[42] Liu X, Chen J, Chen W, Xu Y, Shen Y and Xu X. Targeting IGF2BP3 in cancer. Int J Mol Sci 2023; 24: 9423.
[43] DeBerardinis RJ, Lum JJ, Hatzivassiliou G and Thompson CB. The biology of cancer: metabolic reprogramming fuels cell growth and proliferation. Cell Metab 2008; 7: 11-20.
[44] Monga SP. Role of Wnt/beta-catenin signaling in liver metabolism and cancer. Int J Biochem Cell Biol 2011; 43: 1021-1029.
[45] Valkenburg KC, Graveel CR, Zylstra-Diegel CR, Zhong Z and Williams BO. Wnt/beta-catenin signaling in normal and cancer stem cells. Cancers (Basel) 2011; 3: 2050-2079.
[46] El Wakil A and Lalli E. The Wnt/beta-catenin pathway in adrenocortical development and cancer. Mol Cell Endocrinol 2011; 332: 32-37.
[47] Mohammed MK, Shao C, Wang J, Wei Q, Wang X, Collier Z, Tang S, Liu H, Zhang F, Huang J, Guo D, Lu M, Liu F, Liu J, Ma C, Shi LL, Athiviraham A, He TC and Lee MJ. Wnt/beta-catenin signaling plays an ever-expanding role in stem cell self-renewal, tumorigenesis and cancer chemoresistance. Genes Dis 2016; 3: 11-40.
[48] Ranes M, Zaleska M, Sakalas S, Knight R and Guettler S. Reconstitution of the destruction complex defines roles of AXIN polymers and APC in beta-catenin capture, phosphorylation, and ubiquitylation. Mol Cell 2021; 81: 3246-3261, e3211.
[49] Cheng X, Xu X, Chen D, Zhao F and Wang W. Therapeutic potential of targeting the Wnt/beta-catenin signaling pathway in colorectal cancer. Biomed Pharmacother 2019; 110: 473-481.
[50] Lee R, Li J, Li J, Wu CJ, Jiang S, Hsu WH, Chakravarti D, Chen P, LaBella KA, Li J, Spring DJ, Zhao D, Wang YA and DePinho RA. Synthetic essentiality of tryptophan 2,3-dioxygenase 2 in APC-mutated colorectal cancer. Cancer Discov 2022; 12: 1702-1717.
[51] Wang B, Wang T, Zhu H, Yan R, Li X, Zhang C, Tao W, Ke X, Hao P and Qu Y. Neddylation is essential for beta-catenin degradation in Wnt signaling pathway. Cell Rep 2022; 38: 110538.
[52] Azzolin L, Panciera T, Soligo S, Enzo E, Bicciato S, Dupont S, Bresolin S, Frasson C, Basso G, Guzzardo V, Fassina A, Cordenonsi M and Piccolo S. YAP/TAZ incorporation in the beta-catenin destruction complex orchestrates the Wnt response. Cell 2014; 158: 157-170.

Table S1. shRNA and siRNA sequences

Gene name	Sequence
sh-NC	5'-CCGGTTCTCCGAACGTGTCACGTTTTTCAAGAGAAAACGTGACACGTTCGGAGAATTTTTTGGTACC-3'
sh-CDC5L-1	5'-CCGGTAAATCAGATTCTTTTTTCCTTTCAAGAGAAGGAAAAAAGAATCTGATTTATTTTTTGGTACC-3'
sh-CDC5L-2	5'-CCGGTCTGTAAATCTGTTAAAGGCGTTCAAGAGACGCCTTTAACAGATTTACAGATTTTTTGGTACC-3'
sh-WNT7B-1	5'-CCGGAATCTTGTTGCAGATGATGTTTTCAAGAGAAACATCATCTGCAACAAGATTTTTTTTGGTACC-3'
sh-WNT7B-2	5'-CCGGTCAAAAGAAGGAAAGACGGCATTCAAGAGATGCCGTCTTTCCTTCTTTTGATTTTTTGGTACC-3'
si-NC	5'-UUCUCCGAACGUGUCACGUTT-3
si-METTL14-1	5'-UCCAUUUUGUCUUCAUCUGTT-3'
si-METTL14-2	5'-UGAUAAUUAAGUCAAUGUCTT-3'
si-IGF2BP1-1	5'-UGGAAUAGGUGACAUUCACTT-3'
si-IGF2BP1-2	5'-UCCGUAUUGUACCUAUUGGTT-3'
si-IGF2BP2-1	5'-AGUAGUUCUCAAACUGAUGTT-3'
si-IGF2BP2-2	5'-AUUUUGCUUGGCUUUGAACTT-3'
si-IGF2BP3-1	5'-CGAGGCGCUUUCAGGUAAATT-3'
si-IGF2BP3-2	5'-UCCAGAACGCACUAUUACATT-3'

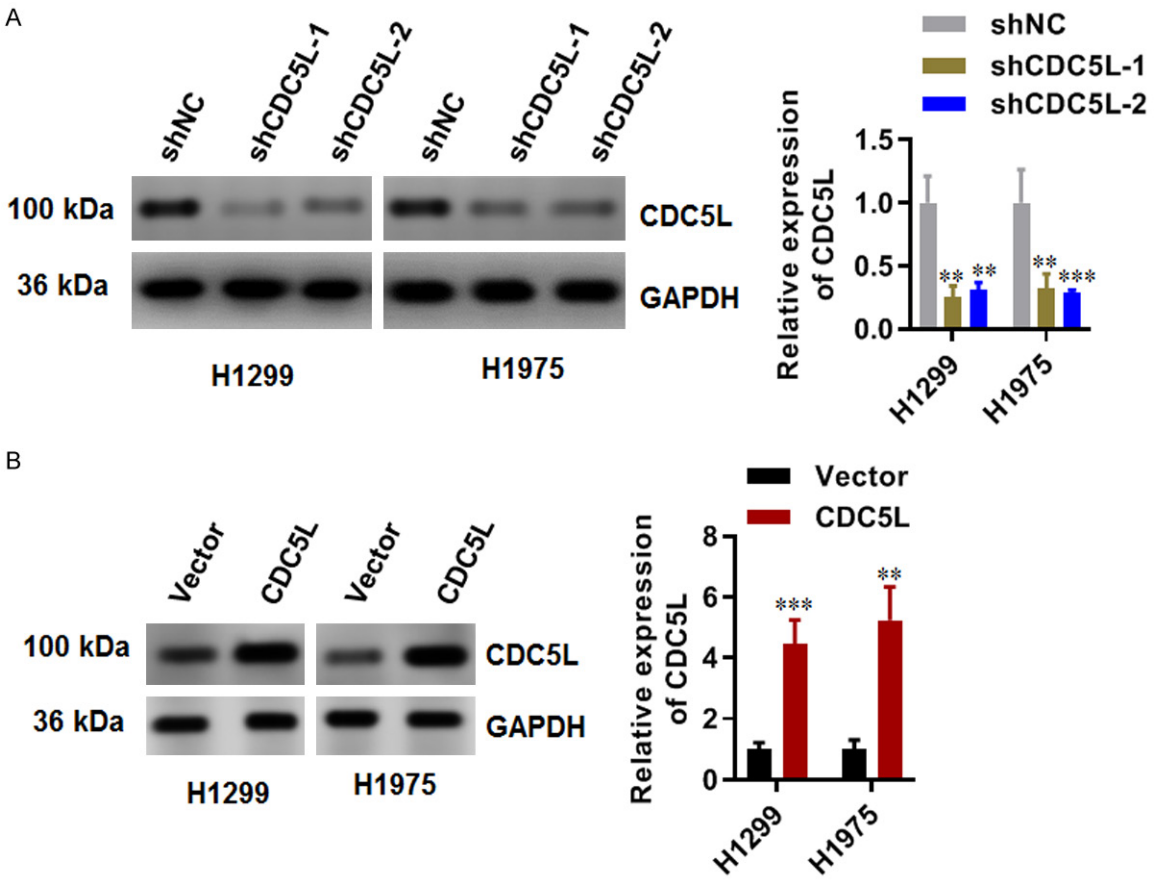

Figure S1. A. Western blot confirmed the knockdown efficiency of CDC5L in H1299 and H1975 cells with 2 different shRNA. shNC, negative control shRNA. B. Western blot confirmed overexpression efficiency in both H1299 and H1975. Data are shown as the mean ± SEM. **P < 0.01, ***P < 0.001.

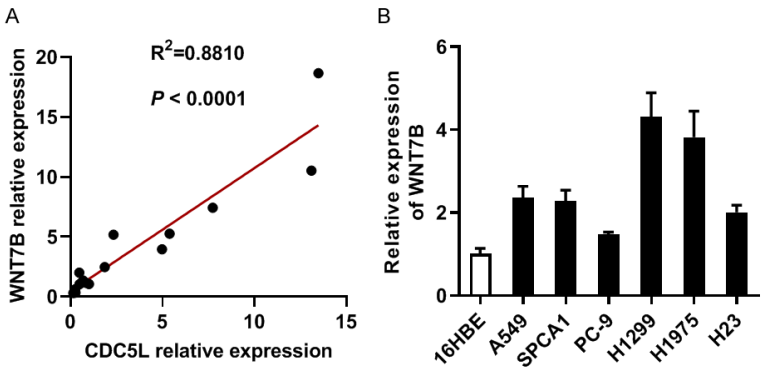

Figure S2. A. CDC5L had a positive correlation with WNT7B (R=0.8810, P < 0.0001). B. qRT-PCR indicated that WNT7B protein is highly expressed in LUAD cell lines.

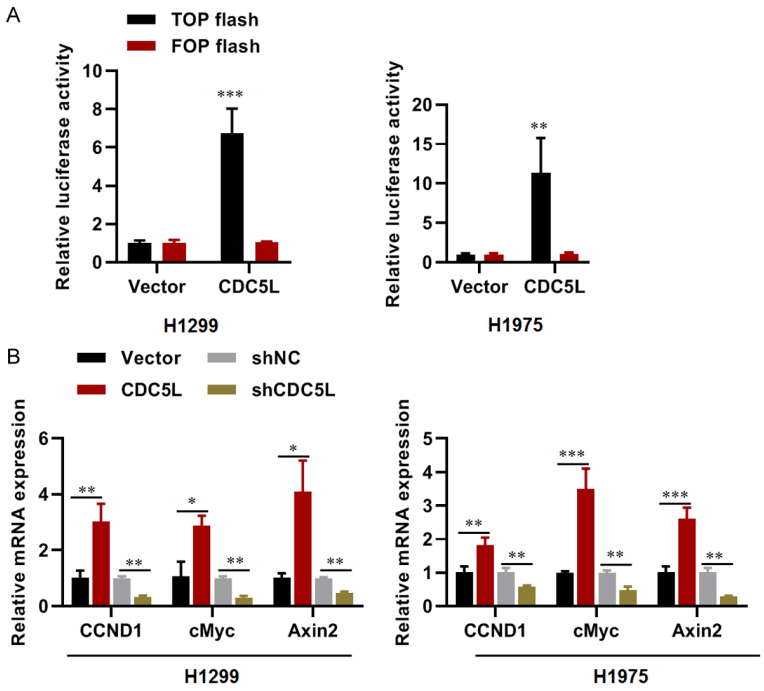

Figure S3. A. Luciferase-reporter assays of TOP/FOP transcriptional activity in the indicated cells. B. qRT-PCR indicated that downregulation of CDC5L decreased but upregulation increased the expression of Wnt/β-catenin downstream genes (CCND1, cMYC, Axin2) in LUAD cells. Data are shown as the mean ± SEM. *P < 0.05, **P < 0.01, ***P < 0.001.

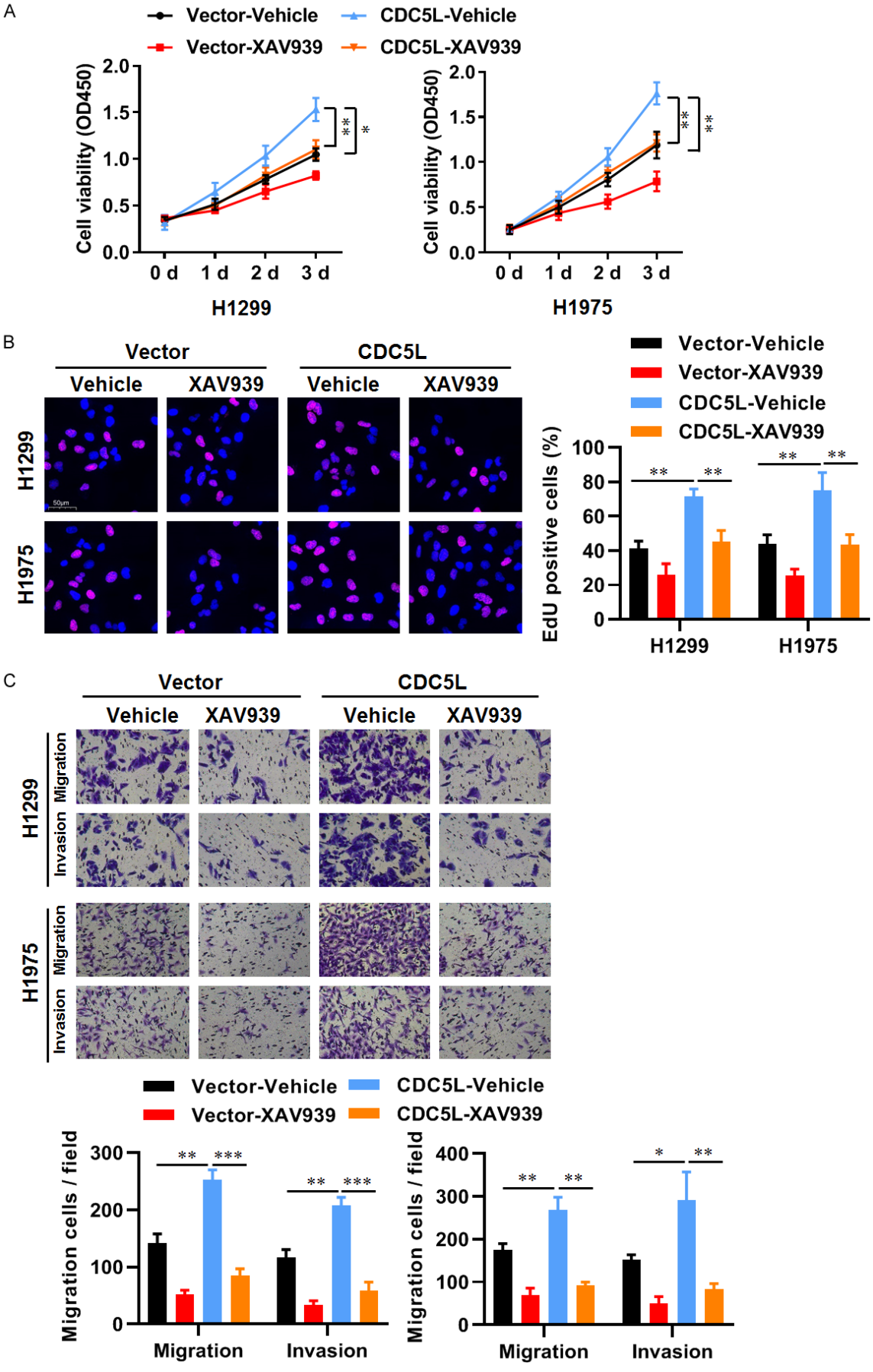
A
Vector-Vehicle
CDC5L-Vehicle
Vector-XAV939
CDC5L-XAV939
Cell viability (OD450)
2.0
1.5
1.0
0.5
0.0
0 d
1 d
2 d
3 d
H1299
H1975
B
Vector
CDC5L
Vehicle
XAV939
H1299
H1975
EdU positive cells (%)
100
80
60
40
20
0
C
Migration
Invasion
Migration cells / field
300
200
100
400
Migration
Invasion

Figure S4. CDC5L promotes proliferation and migration of LUAD through the Wnt/β-catenin pathway. A, B. The cell viability of H1299 and H1975 cells were evaluated by CCK8 assay and EdU assay. C. The cell invasive ability of H1299 and H1975 cells were measured by transwell assay. Data are shown as the mean ± SEM. *P < 0.05, **P < 0.01, ***P < 0.001.

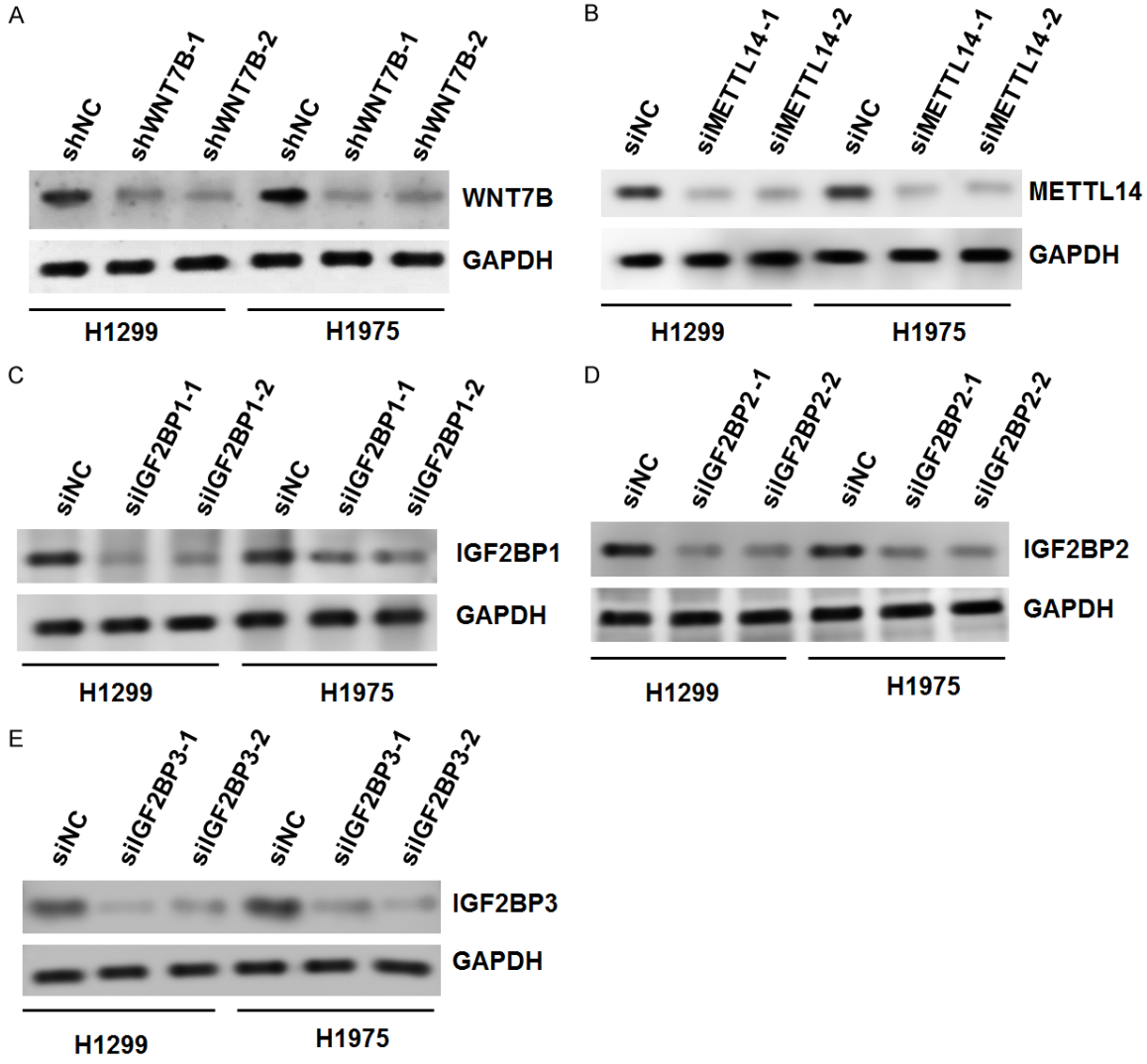

Figure S5. (A) Western blot confirmed the knockdown efficiency of WNT7B (A), METTL14 (B), IGF2BP1 (C), IGF2BP2 (D), and IGF2BP3 (E) in H1299 and H1975 cells with 2 different siRNA or siRNAs. siNC or siNC, negative control siRNA or siRNA.